The Plant Cell, Vol. 28: 3038–3051, December 2016, www.plantcell.org

Orosomucoid Proteins Interact with the Small Subunit of Serine Palmitoyltransferase and Contribute to Sphingolipid Homeostasis and Stress Responses in Arabidopsis[OPEN]

Jian Li,[1] Jian Yin,[1] Chan Rong,[1] Kai-En Li,[1] Jian-Xin Wu,[1] Li-Qun Huang, Hong-Yun Zeng, Sunil Kumar Sahu, and Nan Yao[2]

State Key Laboratory of Biocontrol, Guangdong Provincial Key Laboratory of Plant Resources, School of Life Sciences, Sun Yat-sen University, Guangzhou 510275, P.R. China

Serine palmitoyltransferase (SPT), a pyridoxyl-5′-phosphate-dependent enzyme, catalyzes the first and rate-limiting step in sphingolipid biosynthesis. In humans and yeast, orosomucoid proteins (ORMs) negatively regulate SPT and thus play an important role in maintaining sphingolipid levels. Despite the importance of sphingoid intermediates as bioactive molecules, the regulation of sphingolipid biosynthesis through SPT is not well understood in plants. Here, we identified and characterized the *Arabidopsis thaliana* ORMs, ORM1 and ORM2. Loss of function of both *ORM1* and *ORM2* (*orm1* amiR-*ORM2*) stimulated de novo sphingolipid biosynthesis, leading to strong sphingolipid accumulation, especially of long-chain bases and ceramides. Yeast two-hybrid, bimolecular fluorescence complementation, and coimmunoprecipitation assays confirmed that ORM1 and ORM2 physically interact with the small subunit of SPT (ssSPT), indicating that ORMs inhibit ssSPT function. We found that *orm1* amiR-*ORM2* plants exhibited an early-senescence phenotype accompanied by H_2O_2 production at the cell wall and in mitochondria, active vesicular trafficking, and formation of cell wall appositions. Strikingly, the *orm1* amiR-*ORM2* plants showed increased expression of genes related to endoplasmic reticulum stress and defenses and also had enhanced resistance to oxidative stress and pathogen infection. Taken together, our findings indicate that ORMs interact with SPT to regulate sphingolipid homeostasis and play a pivotal role in environmental stress tolerance in plants.

INTRODUCTION

In eukaryotes, sphingolipids make up ~40% of the lipids of the plasma membrane and are also abundant in other endomembranes. The functions of these key lipids have been intensively investigated in mammals and yeast for decades (Hannun and Obeid, 2008), and recent work has begun to explore sphingolipid biochemistry in plants. Sphingolipids play pivotal roles as membrane structural components, as bioactive molecules involved in signal transduction and cell regulation, and in a wide range of other biological processes, including secretion, programmed cell death, autophagy, stress responses, and cell-cell interactions (Liang et al., 2003; Markham et al., 2011; Sentelle et al., 2012; Bi et al., 2014; Li et al., 2015; Wu et al., 2015). On the outer leaflet of the membrane, sphingolipids form membrane microdomains with cholesterol to provide conformational support for membrane proteins and serve as a platform for recruitment of signaling molecules (Lingwood and Simons, 2010).

In humans, changes in sphingolipid contents have been closely linked to diabetes (Summers and Nelson, 2005), cancer (Modrak et al., 2006), Alzheimer's disease (Mizuno et al., 2016), cardiovascular disease, and respiratory disease (Park et al., 2006). For example, sphingosine-1-phosphate can bind to the G protein-coupled receptor EDG5 to inhibit the activity of Rac protein, which could prevent the metastasis of tumor cells (Okamoto et al., 2000). The sphingosine-1-phosphate analog fingolimod (FTY720) has a similar activity and can be used for cancer treatment (Brinkmann et al., 2010). Sphingolipids also function in plant development and responses to biotic or abiotic stresses (zhen et al., 2006, 2009; Dietrich et al., 2008; Teng et al., 2008; Markham et al., 2011; Ternes et al., 2011; König et al., 2012; Zhang et al., 2013; Bi et al., 2014).

Regulation of the levels of sphingolipids involves the modulation of key enzymes such as ceramide synthases, ceramidases, ceramide kinase, glucosylceramidase, and inositolphosphorylceramidase (Liang et al., 2003; Wang et al., 2008; Ternes et al., 2011; Bi et al., 2014; Li et al., 2015; Msanne et al., 2015; Wu et al., 2015). Serine palmitoyltransferase (SPT) is a pyridoxyl-5′-phosphate-dependent enzyme that catalyzes the first and rate-limiting step in sphingolipid biosynthesis, the condensation between L-serine and a long-chain acyl thioester such as palmitoyl-CoA (C16-CoA) to generate long-chain bases (LCBs) (Chen et al., 2006). In *Arabidopsis thaliana*, the SPT enzyme has three subunits, LCB1, LCB2a, and LCB2b. The *fbr11-2*/*lcb1-1* mutant, a loss-of-function mutation of *LCB1*, shows abnormal development, initiating apoptotic cell death in binucleate microspores, and the *LCB2* loss-function mutant displays gametophytic lethality (Chen et al., 2006; Dietrich et al., 2008; Teng et al., 2008).

Work in animals and yeast showed that orosomucoid (ORM) proteins can modulate SPT activity (Breslow et al., 2010; Han et al., 2010; Gururaj et al., 2013). The ORM family proteins are endoplasmic reticulum (ER)-resident membrane proteins encoded by

[1] These authors contributed equally to this work.
[2] Address correspondence to yaonan@mail.sysu.edu.cn.
The author responsible for distribution of materials integral to the findings presented in this article in accordance with the policy described in the Instructions for Authors (www.plantcell.org) is: Nan Yao (yaonan@mail.sysu.edu.cn).
[OPEN]Articles can be viewed without a subscription.
www.plantcell.org/cgi/doi/10.1105/tpc.16.00574

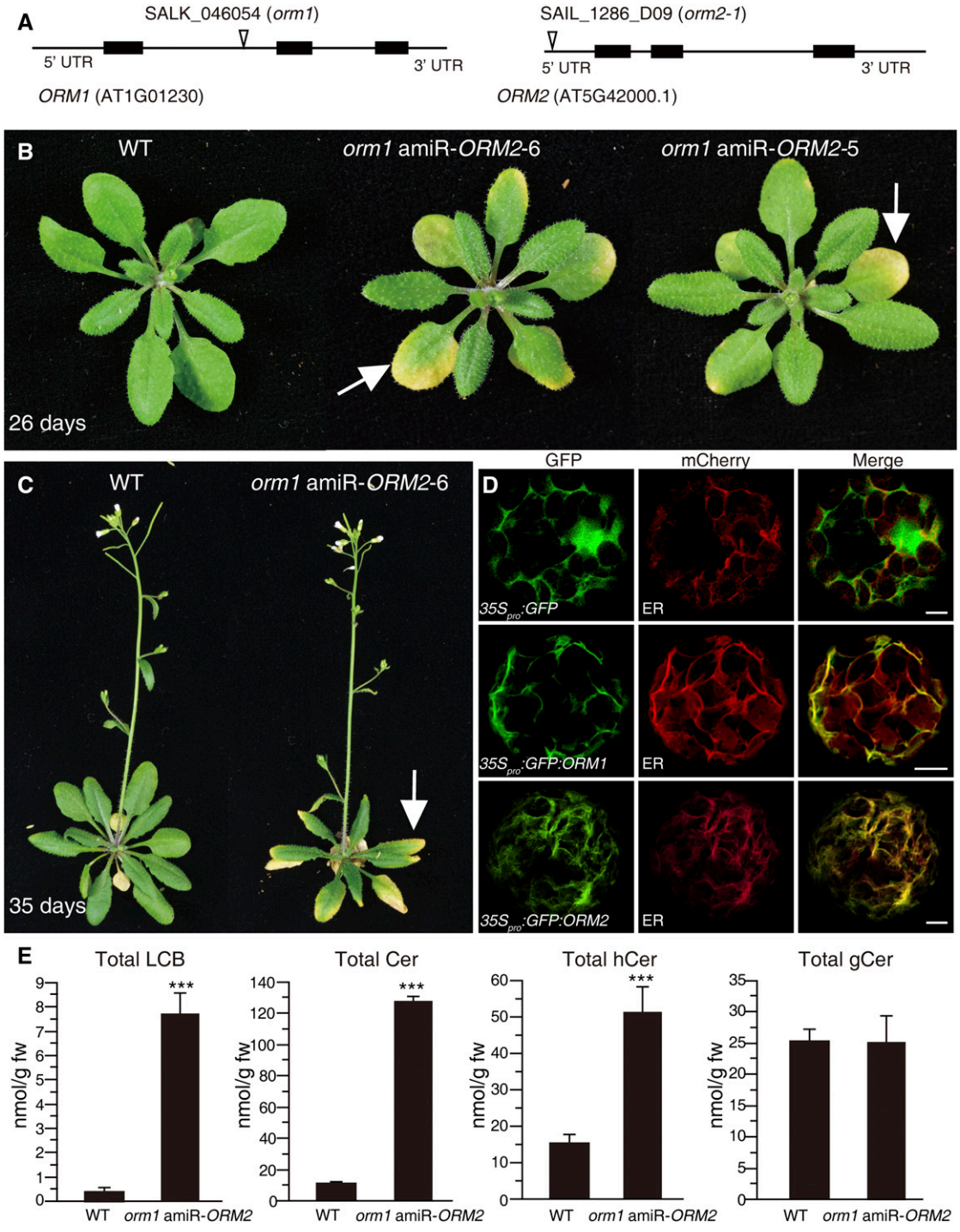

Figure 1. Loss of Function of *ORM1* and *ORM2* Causes an Early-Senescence Phenotype and Sphingolipid Accumulation.

(A) The structures of Arabidopsis *ORM1* and *ORM2* and the locations of T-DNA insertions.
(B) and **(C)** The phenotype of wild-type and *ORM* loss-of-function plants at 26 **(B)** and 35 **(C)** d old. The white arrows indicate leaf senescence in *orm1* amiR-*ORM2* plants.
(D) Subcellular localization of ORM proteins. The fusion constructs $35S_{pro}$:*GFP-ORM1* and $35S_{pro}$:*GFP-ORM2* were coexpressed with the ER mCherry marker (TAIR, CD3-960) by transient expression in protoplasts. The $35S_{pro}$:*GFP* construct and CD3-960 were cotransformed as controls. The images were obtained by confocal microscopy after 16 h incubation. The experiments were repeated at least three times with similar results. Bars = 5 μm.

ORM or *ORMDL* genes, which are conserved from yeast to humans (Hjelmqvist et al., 2002; Moffatt et al., 2007). Depletion of the mammalian ORMDL1-3 eliminates the feedback of exogenous ceramide on ceramide biosynthesis, indicating that ORMDL proteins function as the primary regulators of ceramide biosynthesis in mammalian cells (Siow and Wattenberg, 2012). In yeast, genetic studies established a link between *ORM1* and *ORM2* and sphingolipid metabolism, as deletion of *ORM1* and *ORM2* leads to toxic accumulation of sphingolipids, whereas overexpression of *ORM1* or *ORM2* leads to reduced sphingolipid levels (Breslow et al., 2010). Thus, *ORM1* and *ORM2* negatively regulate sphingolipid synthesis.

Yeast (*Saccharomyces cerevisiae*) Orm proteins regulate sphingolipid metabolism by forming a multiprotein complex with SPT, termed the SPOTS complex, which also contains the SPT accessory subunit Tsc3 and the phosphoinositide phosphatase Sac1. Phosphorylation of Orm proteins, mediated by both branches of the TOR signaling pathway, regulates SPT activity to maintain sphingolipid homeostasis (Breslow et al., 2010; Han et al., 2010; Breslow, 2013). The Ypk1 protein kinase, downstream of rapamycin complex TORC, regulates Orm1 and Orm2 phosphorylation (Roelants et al., 2011; Berchtold et al., 2012; Niles et al., 2012; Sun et al., 2012; Shimobayashi et al., 2013). Orm proteins' SPT-inhibitory activity is subject to feedback regulation by multiple sphingolipid intermediates, including LCBs, ceramide, and complex sphingolipids. When sphingolipid biosynthesis is disrupted, phosphorylation of their amino termini activates Orm1 and Orm2, thus enabling a compensatory increase in SPT activity (Breslow et al., 2010; Liu et al., 2012). Orm1 activity is adjusted in response to manipulation of *Orm2* expression levels, with increased *Orm2* expression causing a corresponding increase in Orm1 phosphorylation and vice versa. Phosphoregulation of Orm proteins controls sphingolipid biosynthesis in response to various stresses, including heat stress, ER stress, iron stress, and cell wall stress (Sun et al., 2012; Lee et al., 2012; Gururaj et al., 2013).

In addition to ORM, eukaryotes have a class of polypeptides, the SPT small subunits (ssSPT), which can regulate SPT activity. For example, yeast has an 80-amino acid polypeptide called Tsc3, which combines with the LCB1 and LCB2 subunits to form a trimer, thereby activating SPT (Gable et al., 2000). Humans have two ssSPT: ssSPTa (68 amino acids) and ssSPTb (76 amino acids). Coexpression of human ssSPTa or ssSPTb and LCB1, LCB2a, or LCB2b can activate SPT in yeast *lcb1 lcb2*△ mutants (Han et al., 2009). Recent work reported that Arabidopsis has two ssSPTs, encoded by *ssSPTa* (At1g06515) and *ssSPTb* (At2g30942). These 56-amino acid ssSPTs can activate SPT and play an important role in the formation of mature pollen (Kimberlin et al., 2013).

Considerable progress has been made in advancing our knowledge of plant sphingolipid metabolism in the past 10 to 15 years. However, our understanding of ORMs, particularly in plants, remains in its infancy. Here, we reported functional characterization of the ORM genes (*ORM1*, AT1G01230; *ORM2*, AT5G42000) in Arabidopsis. We discovered that ORM can interact with and inhibit ssSPT, thus affecting sphingolipid levels. Our studies strongly suggest that ORM plays a key role in the plant response to biotic and abiotic stress.

RESULTS

Loss of ORM1 and ORM2 Function Causes an Early-Senescence Phenotype and High Sphingolipid Accumulation

ORM family genes encode conserved ER membrane proteins in eukaryotic cells. Arabidopsis has two genes encoding homologs of *S. cerevisiae* Orm, AT1G01230 and AT5G42000, designated *ORM1* and *ORM2* (Figure 1A), which encode 157- and 154-amino acid polypeptides with 39 and 35% identity to Orm1 in yeast, respectively (Supplemental Figure 1A). Using the TMHMM protein structure analysis tool (http://www.cbs.dtu.dk/services/TMHMM/), we found that ORM1 and ORM2 have three predicted transmembrane domains (Supplemental Figure 2). The N-terminal extension found in yeast was absent from Arabidopsis ORMs, but phosphorylation site analysis (using NetPhos and the plant-specific algorithm PhosPhAt) showed ORM1 and ORM2 to have possible phosphorylation sites (Supplemental Figure 1A). *ORM1* and *ORM2* were expressed at higher levels in siliques than in other tissues (Supplemental Figure 1B). Our confocal microscopy observations confirmed that ORM1 and ORM2 localized to the ER of Arabidopsis (Figure 1D).

To test the function of the Arabidopsis ORMs, we characterized the available T-DNA mutant lines for these genes: SALK_046054 (predicted T-DNA insertion in the first intron of *ORM1*) and SAIL_1286_D09 (predicted T-DNA insertion in the 5′ untranslated region of *ORM2*). Homozygous lines were identified for each of these mutants. We did not detect the full-length transcript of *ORM1* in SALK_046054, indicating that the line is a null mutant (Supplemental Figures 1C and 1E). In Arabidopsis, according to TAIR (http://www.arabidopsis.org), *ORM2* has two splice isoforms, AT5G42000.1 and AT5G42000.2. However, our RT-PCR experiments detected only the transcripts of AT5G42000.1 (*ORM2.1*) in plants (Supplemental Figure 1D). Since the full-length transcript of *ORM2* was still detected in SAIL_1286_D09 (Supplemental Figure 1D), we also generated an artificial microRNA (amiR) line targeting *ORM2* (amiR-*ORM2*) (Supplemental Figure 1E). For subsequent analysis, we crossed *orm1* with amiR-*ORM2* plants and obtained the *orm1* amiR-*ORM2* homozygous

Figure 1. (continued).

(E) Sphingolipids accumulated in *orm1* amiR-*ORM2* plants. Sphingolipids were extracted from 28-d-old plants following the steps described in Methods. The main sphingolipids were separated and identified by HPLC-ESI-MS. The amount of total LCBs, ceramides (Cer), hydroxyceramides (hCer), and glucosylceramides (gCer) was quantified (see Supplemental Figure 4 for major LCB and ceramide species). The experiment was repeated three times with similar results using independent samples. Values are means ± SE from three technical replicates. Asterisks show a significant difference from the wild type using Student's *t* test (***$P < 0.001$).

lines. In addition, we placed *ORM1* or *ORM2* cDNAs under control of the CaMV35S promoter to create the overexpression lines *ORM1-OX* and *ORM2-OX* in Arabidopsis (Supplemental Figures 1C and 1D). The *orm1* amiR-*ORM2* plants initially underwent the same development as the wild type (Supplemental Figure 3A, top panel; *orm1* amiR-*ORM2-6* and *orm1* amiR-*ORM2-5*). However, in late development, the *orm1* amiR-*ORM2* plants showed accelerated senescence, characterized by early chlorosis of rosette leaf tips (Figures 1B and 1C). By contrast, the development of the *orm1* single mutant and amiR-*ORM2* plants was similar to that of wild-type plants (Supplemental Figure 3A).

In yeast, Orm proteins act as negative mediators of sphingolipid biosynthesis by inhibiting SPT activity (Han et al., 2010). To determine the role of ORM1 and ORM2 in the regulation of sphingolipid biosynthesis in Arabidopsis, we comprehensively analyzed the major classes of sphingolipids in *orm1* and amiR-*ORM2* plants. We observed no obvious changes in sphingolipids in *orm1* and amiR-*ORM2* plants compared with the wild type (Supplemental Figure 3B). However, the sphingolipid profile of 28-d-old *orm1* amiR-*ORM2* plants showed a dramatic increase in the total sphingolipid contents, especially in LCBs (~15-fold) and ceramides (8-fold), compared with the wild type. By contrast, the amount of glucosylceramides did not change relative to the wild type (Figure 1E). Among LCBs, we noticed that d18:0 LCB showed the largest difference in *orm1* amiR-*ORM2* (Supplemental Figure 4). Remarkably, the ceramide backbones containing long-chain fatty acids (C16) exhibited a more dramatic increase than ceramide containing very-long-chain fatty acids (C20, C24, and C26) (Supplemental Figure 4).

We also measured the sphingolipid contents of *orm1* amiR-*ORM2* and wild-type rosettes at different developmental stages, and the results showed a gradual accumulation of sphingolipids in *orm1* amiR-*ORM2* plants (Supplemental Figure 5). The sphingolipid profile of 21-d-old plants revealed that the total amounts of LCBs, ceramides, and hydroxyceramides were higher in *orm1* amiR-*ORM2* plants compared with wild-type plants. However, no visible early-senescence phenotype was observed in the *orm1* amiR-*ORM2* plants at this stage (Supplemental Figure 3). In other words, *orm1* amiR-*ORM2* plants accumulated sphingolipids prior to the early senescence. There were no significant changes in sphingolipids in *orm1* mutants, amiR-*ORM2* plants, or overexpression transgenic plants with respect to wild-type plants at different developmental stages (Supplemental Figures 3 and 5). These results indicated that ORM1 and ORM2 negatively coregulate sphingolipid biosynthesis in plants. In addition, the early-senescence phenotype of *orm1* amiR-*ORM2* plants was associated with overaccumulation of sphingolipids.

ORMs Suppress the de Novo Biosynthesis of Sphingolipids in Arabidopsis

To decipher the possible cause of the overaccumulation of sphingolipids, we used ^{15}N-labeling and metabolic turnover analysis to directly measure in vivo sphingolipid changes, as we reported previously (Shi et al., 2015). Seven-day-old *orm1* amiR-*ORM2* and wild-type seedlings were transferred to N-deficient 0.5× Murashige and Skoog (MS) liquid medium containing 5 mM ^{15}N-serine in a time course. Isotope-labeled LCBs and ceramides of *orm1* amiR-*ORM2* plants accumulated to significant levels after 24 h of incubation with ^{15}N-serine, relative to wild-type and *orm1*

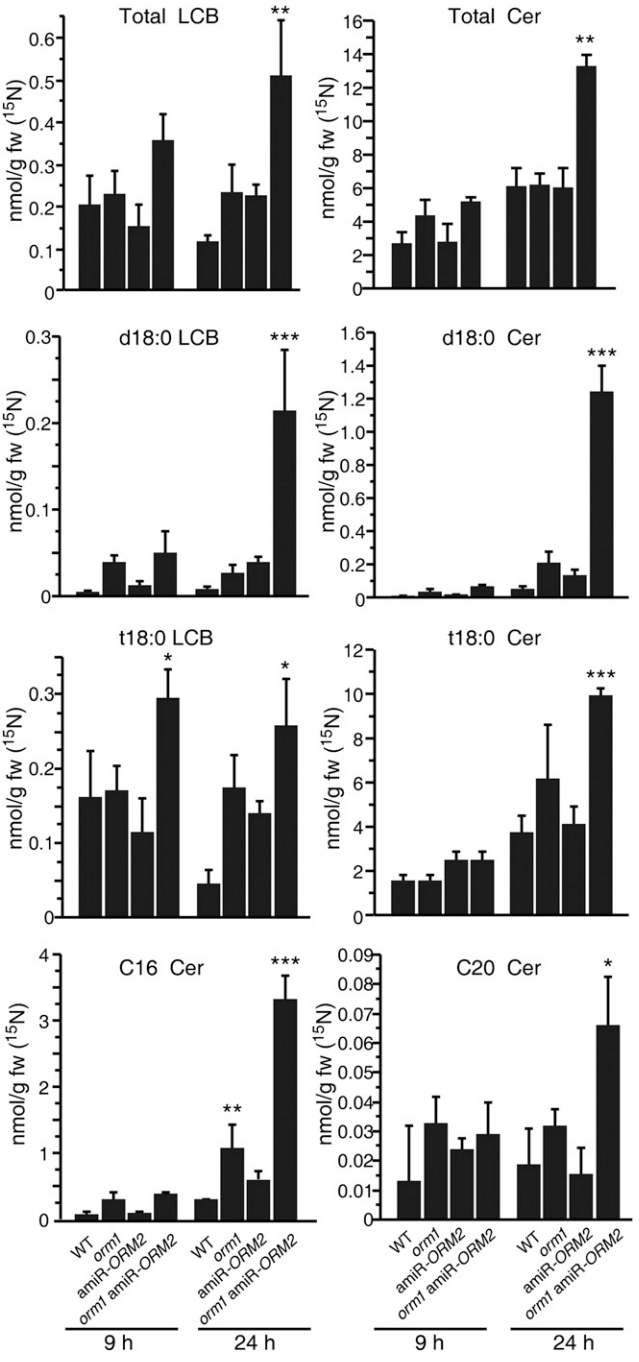

Figure 2. ORM Suppresses the de Novo Biosynthesis of Sphingolipids in Arabidopsis.

Seven-day-old wild-type, *orm1*, amiR-*ORM2*, and *orm1* amiR-*ORM2* seedlings were transferred to 5 mM ^{15}N-serine labeled N-deficient 0.5× MS liquid medium for 9 to 24 h. Sphingolipids were then extracted and measured as described in Methods. Note that except total LCB and total ceramides (top panels), major LCB and ceramide species significantly increased at 24 h in *orm1* amiR-*ORM2* seedlings. Error bars represent the means ± SE from triplicate biological repeats. Asterisks show a significant difference from the wild type using Student's *t* test (*$P < 0.05$, **$P < 0.01$, and ***$P < 0.001$).

or amiR-*ORM2* plants (Figure 2). It is noteworthy that the increase of ^{15}N-labeled d18:0 LCB was greater than that of t18:0 LCB (Figure 2). In addition to quantitative changes in ceramides, d18:0 ceramides showed a more dramatic increase than t18:0 ceramides (Figure 2). The initial LCB produced in plants is dihydrosphingosine (d18:0 LCB) (Chen et al., 2009). Hence, these measurements confirmed our hypothesis that the loss of ORM1 and ORM2 function in the *orm1* amiR-*ORM2* plants promotes the de novo biosynthesis of sphingolipids and ultimately leads to higher accumulation of sphingolipids. Moreover, the higher levels of ^{15}N-labeled ceramides containing C16 fatty acid in *orm1* amiR-*ORM2* plants (Figure 2) were consistent with accumulation of C16 ceramides in 28-d-old *orm1* amiR-*ORM2* plants (Supplemental Figure 4).

ORM1 and ORM2 Interact with ssSPT

Previous studies in yeast and mammals showed that ORM proteins physically interact with Lcb1 and Lcb2 (Han et al., 2010). To test the interactions of ORM proteins in Arabidopsis, we first applied yeast two-hybrid assays. Surprisingly, our yeast two-hybrid assays revealed that the ORM proteins physically interact with the ssSPT (Figure 3A). The interaction was further confirmed by coimmunoprecipitation (co-IP) assays. Anti-Flag resins could precipitate not only ORM-Flag but also GFP-ssSPT (Figure 3B). When free GFP was used as a control, no GFP signals were detected in the eluate (Figure 3B). We also used bimolecular fluorescence complementation (BiFC) assays to confirm the ORM-ssSPT interaction. Clear YFP fluorescence was observed in protoplasts co-transformed with *pSATN-nEYFP-ORM1* and *pSATN-cEYFP-ssSPTa* or *pSATN-cEYFP-ssSPTb*, *pSATN-nEYFP-ORM2*, and *pSATN-cEYFP-ssSPTa* or *pSATN-cEYFP-ssSPTb* constructs (Figure 3C). However, no YFP signal was detected in the protoplasts co-transformed with one construct in combination with an empty vector (Figure 3C). In addition, our confocal microscopy observations confirmed that ssSTPa and ssSTPb also localized to the ER where they interact with ORMs (Supplemental Figure 6). These results

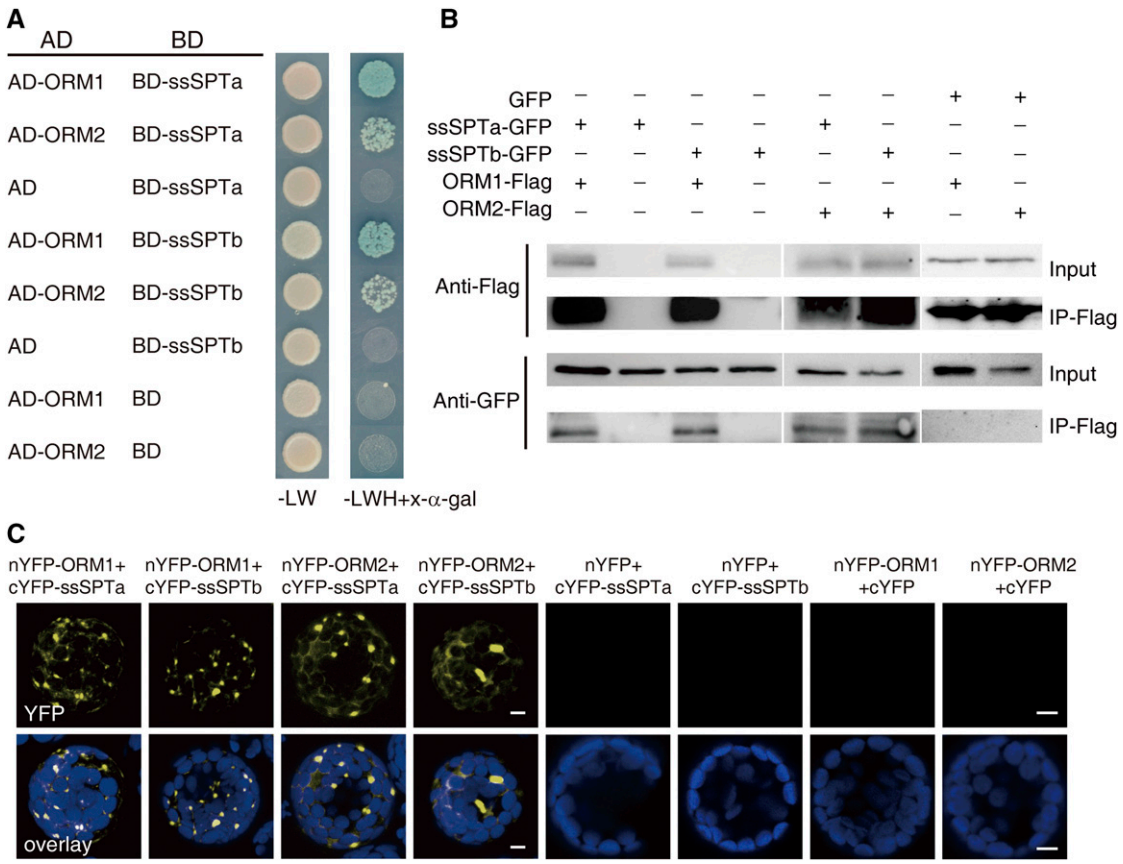

Figure 3. Physical Interaction between ORM and ssSPT.

(A) Yeast two-hybrid assay showing that ssSPTa and ssSPTb interact with ORM1 and ORM2. Vectors pGADT7 (AD) and pGBKT7 (BD) were used as negative controls.

(B) Co-IP assays of ORM1, ORM2, ssSPTa, and ssSPTb in protoplasts. Flag-tagged ORM1 and ORM2 were immunoprecipitated with an anti-Flag antibody, and coimmunoprecipitated ssSPTa-GFP and ssSPTb-GFP were detected by an anti-GFP antibody. The "+" or "−"denote the presence or absence of the protein in each sample. Free GFP was used as a negative control.

(C) BiFC interaction of ssSPTa and ORM1, ssSPTb and ORM2, ssSPTa and ORM2, and ssSPTb and ORM2 in Arabidopsis leaf protoplasts. Overlaid images show signals for YFP (yellow) and chloroplasts (blue). Empty vectors were used as negative controls. Bars = 5 μm.

are consistent with the physical interaction of ORM1 and ORM2 with ssSPTa and ssSPTb at the ER. We also found that SPTs localized to ER in the *orm1* amiR-*ORM2* plants, as confirmed by transient coexpression with *35S$_{pro}$:EGFP-LCB1* or *35S$_{pro}$:EGFP-LCB2a/b* and an ER marker, suggesting that loss of function of ORMs did not affect subcellular localization of the SPT complex (Supplemental Figure 7).

ORM Proteins Decrease the Biosynthesis of Sphingolipids

Reduced SPT activity may decrease sensitivity to fumonisin B1 (FB1) by decreasing levels of cytotoxic LCBs, whereas increased SPT activity may increase sensitivity to FB1 by increasing the levels of LCBs (Shi et al., 2007; Saucedo-García et al., 2011). ssSPTa/ssSPTb can strongly stimulate SPT activity and increase the production of LCBs in Arabidopsis (Kimberlin et al., 2013). To explore the function of Arabidopsis ORMs, we grew plants on agar plates with FB1 to test the significance of the interaction between ORM and ssSPT. Both *ORM1-OX* and *ORM2-OX* overexpression lines showed resistance to 0.5 μM FB1, whereas the *orm1* amiR-*ORM2* plants were highly sensitive to FB1 (Figure 4). Consistent with a previous human ORM study (Breslow et al., 2010), ORM proteins thus appear to negatively regulate sphingolipid biosynthesis.

Loss of ORM Proteins Increases ER Stress-Related Responses

To understand whether the loss of ORM proteins affects cellular ultrastructure, we fixed the *orm1* amiR-*ORM2* leaves before the appearance of the senescence phenotype. As shown in Figure 5, compared with the normal nuclei observed in the wild-type cells (Figure 5A), the *orm1* amiR-*ORM2* cells showed condensed chromatin aggregated in the perinuclear membrane, which indicates dying cells (Figure 5B; Liang et al., 2003), and a large amount of tiny membrane sacs close to the plasma membrane and the cell wall (Figures 5C and 5D). Interestingly, we found a large cell wall apposition, a clear marker of the defense response, in the *orm1* amiR-*ORM2* leaf cells (Figure 5E). When we used the cerium chloride method (Bi et al., 2014) to detect reactive oxygen species (ROS), we observed H_2O_2 production on the cell wall (Figures 5G and 5H), the cytosolic area close to the apoplast (Figure 5I) and in the mitochondria (Figure 5J). No cerium deposits were observed in the wild-type control (Figure 5F). In the dying cells, irregular ER and vacuolization were frequently observed (Figure 5K). These observations suggest that loss of ORMs may induce active vesicular trafficking around the plasma membrane, and this ER stress phenomenon is associated with defense responses.

To support the transmission electron microscopy (TEM) observations, we investigated the expression of genes related to ER stress and defenses. Strikingly, the expression of ER stress marker genes (*bZIP28*, *bZIP60*, *IRE1a*, and *TBF1*) significantly increased in *orm1* amiR-*ORM2* plants, compared with the wild type (Figure 6A). To determine whether the transcription of defense-related genes was affected in plants with decreased ORM function, we analyzed the expression of salicylic acid-related and pathogenesis-related (*PR*) genes in wild-type and *orm1* amiR-*ORM2* plants using RT-qPCR. The *orm1* amiR-*ORM2* plants showed high transcript levels of these genes, such as *PAD4*, *SID2*, and *NPR1*, compared with the wild type (Figure 6B). *PR1* showed especially dramatic enhancement, which is highly linked to the formation of cell wall appositions. No obvious changes of those genes were detected in *orm1* and amiR-*ORM2* plants (Figure 6).

Loss of ORM Proteins Enhances Plant Resistance to Abiotic and Biotic Responses

Recent studies have shown that sphingolipids are involved in plant stress responses (Wang et al., 2008; Peer et al., 2010; Bi et al.,

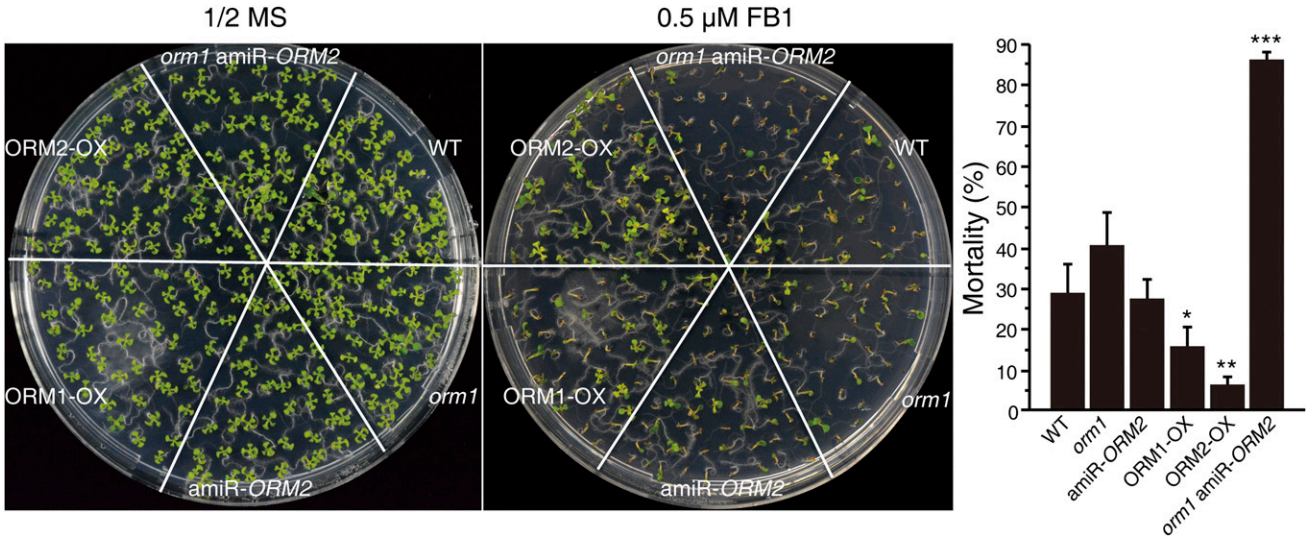

Figure 4. Phenotypes of Wild-Type and *ORM* Transgenic Seedlings after FB1 Treatments.

Seedlings of wild-type, *orm1*, amiR-*ORM2*, and *orm1* amiR-*ORM2* plants and overexpression lines (ORM1-OX and ORM2-OX) were grown on 0.5× MS with or without 0.5 μM FB1 for 9 d and then photographed. Percentage of seedling mortality after 0.5 μM FB1 treatment is shown in the right panel. Asterisks show a significant difference from the wild type using Student's *t* test (*P < 0.05, **P < 0.01, and ***P < 0.001).

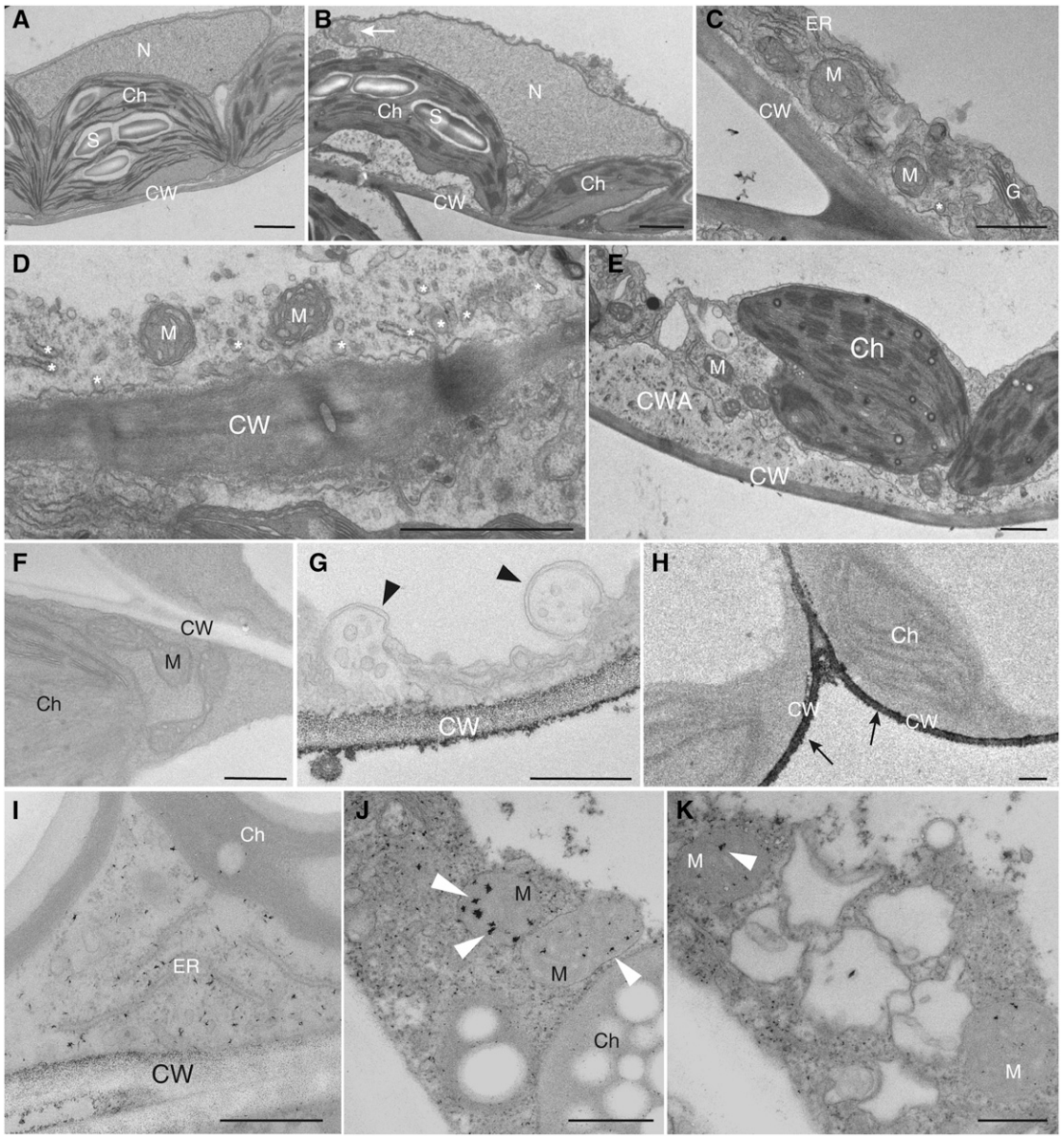

Figure 5. Ultrastructural Features of *orm1* amiR-*ORM2* Leaves.

(A) to **(E)** Representative TEM images of ultrastructure of 25-d-old wild-type **(A)** and *orm1* amiR-*ORM2* (**[B]** to **[E]**) leaves. Note an aggregate of condensed chromatin (**[B]**, white arrow), abnormal ER with loose structure **(C)**, and many small bubbles (**[C]** and **[D]**, white stars) around the plasma membrane and cell wall and a large cell wall apposition in the *orm1* amiR-*ORM2* leaf cell **(E)**.

(F) to **(K)** H_2O_2 production in wild-type **(F)** and *orm1* amiR-*ORM2* (**[G]** to **[K]**) leaves observed by TEM using the histochemical cerium chloride method.

(F) No cerium deposits were observed in the representative wild-type control cell.

(G) and **(H)** Cerium deposits in the plasma membrane and cell wall (black arrows). Note vesicular bodies with double membrane (black arrowheads).

(I) Cerium deposits around the ER close to the cell wall.

(J) and **(K)** H_2O_2 inside mitochondria (**[J]**, white arrowheads) and irregular vacuolization **(K)**.

Ch, chloroplast; CW, cell wall; CWA, cell wall apposition; G, Golgi; M, mitochondrion; N, nucleus; S, starch grain. Bars = 500 nm.

2014; Li et al., 2015). The *orm1* amiR-*ORM2* plants exhibit highly induced expression of ER stress and salicylic acid-related genes, which suggested to us that we should explore the role of ORMs during abiotic and biotic stress. We first treated the *orm1* amiR-*ORM2* plants with the oxidative stress agent methyl viologen (MV), which produces ROS. Surprisingly, *orm1* amiR-*ORM2* plants proved to be tolerant to ROS and exhibited dramatically higher survival rates than wild type (Figures 7A and 7B).

We further inoculated *orm1* amiR-*ORM2* plants with the bacterial pathogen *Pseudomonas syringae* strain DG3. The *orm1*

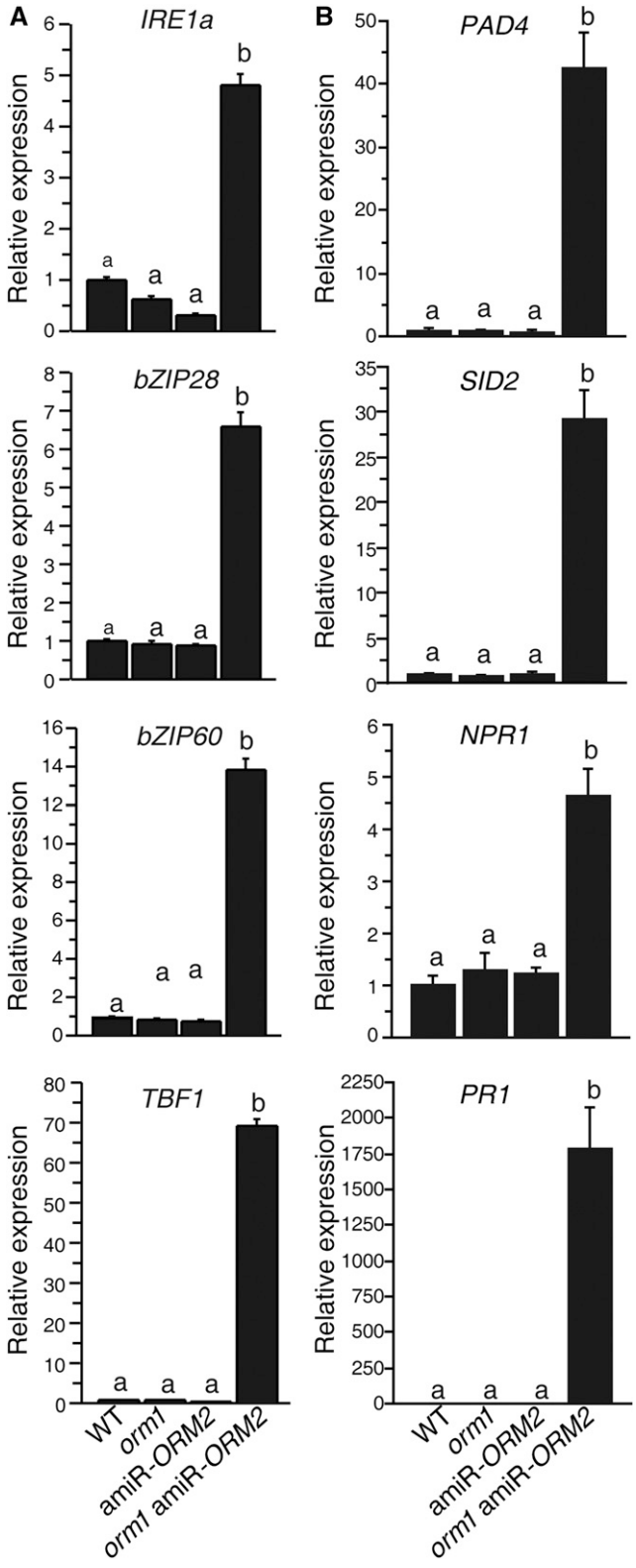

Figure 6. Expression of Genes Related to ER Stress and Defense in *orm1* amiR-*ORM2* Plants.

Approximately 26-d-old wild-type, *orm1*, amiR-*ORM2*, and *orm1* amiR-*ORM2* plants were used to monitor the expression of indicated genes by RT-qPCR. *IRE1a* (At2G17520), *bZIP28* (At3G10800), *bZIP60* (At1G42990), *TBF1* (At4G36990), *PR1* (At2g14610), *PAD4* (At3g52430), *SID2* (At1g74710), and *NPR1* (At1g64280) were used for analysis. *ACT2* transcript levels were used as the internal control. ER stress-related genes **(A)** and salicylic acid pathway-related genes **(B)**. Gene expression values are presented relative to average wild-type levels (set to 1). Samples were analyzed in triplicate biological repeats with similar results. Bars indicate ± SE from three technical replicates. Different letters represent a significant difference from the wild type using a post hoc multiple *t* test ($P < 0.001$).

amiR-*ORM2* plants showed subtle symptoms after infection and proved to be relatively resistant to DG3 bacteria when compared with the wild type (Figure 7C). This enhanced disease resistance was consistent with the detection of high transcript levels of resistance genes in *orm1* amiR-*ORM2* plants. These results indicate that loss of ORM function in Arabidopsis affects the plant's response to abiotic and biotic stress.

DISCUSSION

The ORM proteins, encoded by *ORMDL* (*ORM*) genes, are highly conserved eukaryotic transmembrane proteins located in the ER (Hjelmqvist et al., 2002; Han et al., 2010). The three ORMDL proteins are highly conserved in humans and yeast has two homologous *ORM* genes (*ORM1* and *ORM2*) with redundant functions. Compared with other organisms, the extent of conservation of ORM function in plants remains unclear. In this report, we characterized the two *ORM* genes found in Arabidopsis. Our results indicate that Arabidopsis ORMs function to regulate sphingolipid biosynthesis in maintaining sphingolipid homeostasis and play a role in response to abiotic and biotic stresses.

ORM proteins have few conserved regions, mainly located in the middle of the amino acid sequence, and are generally predicted to form two to four transmembrane domains. The amino acid sequences of the Arabidopsis ORMs share 81% identity and also share 35 to 39% identity with *S. cerevisiae* Orm1 and Orm2 (Supplemental Figure 1), but interestingly, the Arabidopsis isoforms are N-terminally truncated relative to the yeast proteins and therefore lack the three serine residues that are phosphorylated by Ypk1 in the yeast proteins (Roelants et al., 2011). Although we found some possible phosphorylation sites in Arabidopsis ORM1 and ORM2, we still do not know whether the ORMs in Arabidopsis are regulated by phosphorylation, similar to yeast Orm proteins. Another possibility is that Arabidopsis ORMs may be regulated by an allosteric effect on the ORM proteins themselves, where sphingolipids trigger a change in conformation within a preexisting ORM/SPT complex rather than enhancing formation of the complex (Kiefer et al., 2015).

Orm1 and 2 negatively regulate SPT, activating or inhibiting its activity through phosphorylation and dephosphorylation (Tafesse and Holthuis, 2010). Regulation of sphingolipids and Orm proteins involves a feedback mechanism; Orms regulate SPT and sphingolipid metabolites such as LCBs, ceramide, and accumulated

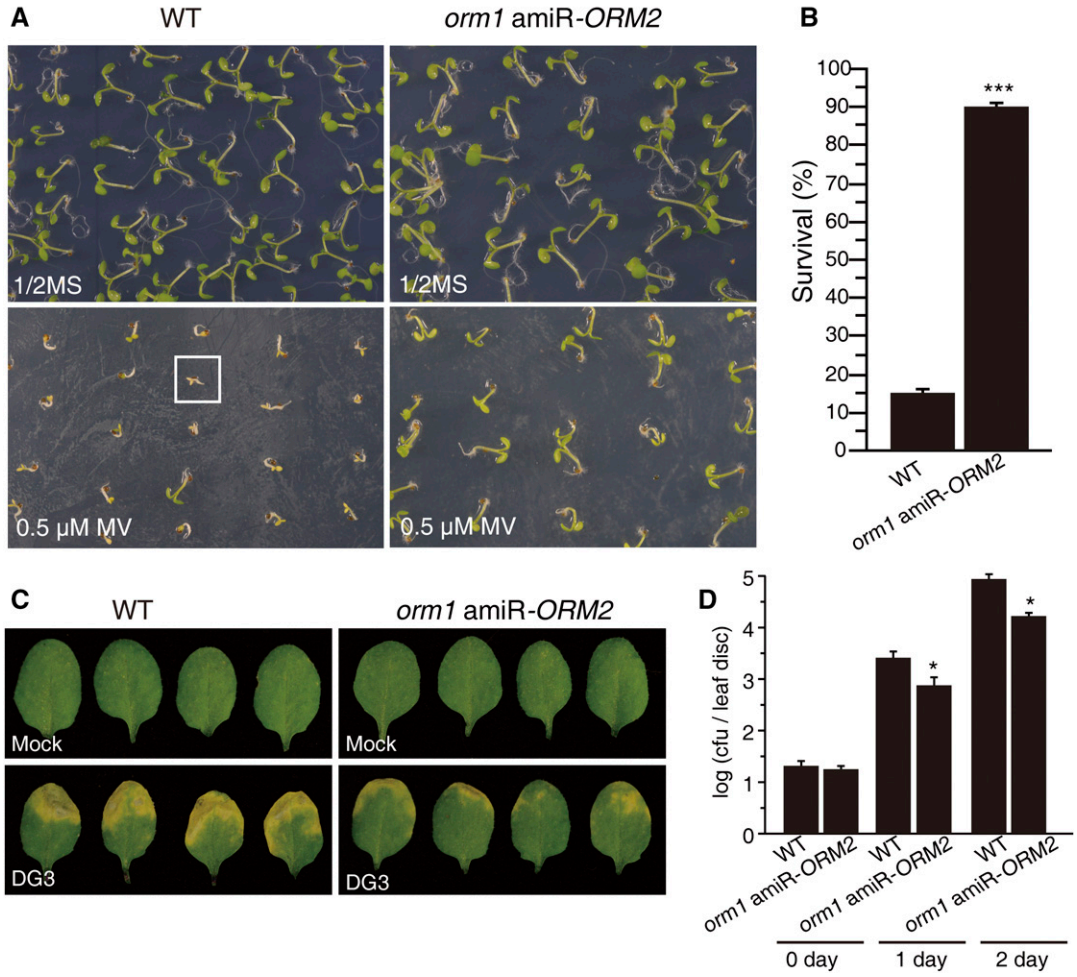

Figure 7. Loss of ORM Protein Enhances the Resistance to Abiotic Stress and Biotic Stress.

(A) The phenotype of wild-type and mutant seedlings after MV treatments. Seedlings were grown on 0.5× MS with or without 0.5 μM MV for 7 d and then photographed. The white square indicates one seedling with a severe phenotype.

(B) Percentage of seedlings with a severe phenotype after 0.5 μM MV treatments. At least 350 seedlings were counted in each genotype. Values represent means ± SE from two independent experiments.

(C) Cell death symptom after infection by *P. syringae* virulent strain DG3 at OD_{600} = 0.005 for 3 d. $MgSO_4$ as a mock-inoculated control was used.

(D) Growth of *P. syringae* virulent strain DG3 in wild-type and *orm1* amiR-*ORM2* plants after infection at OD_{600} = 0.001. Lesion-free plants were inoculated with bacteria at 3 weeks of age. The mean value of the growth of bacteria in nine leaves is indicated in each case. Bars indicate standard deviations. This experiment was repeated three times with similar results. Asterisks show a significant difference from the wild type using Student's *t* test (*P < 0.05).

sphingoid intermediates, and then trigger Orm dephosphorylation, which in turn downregulates sphingolipid biosynthesis (Sun et al., 2012). In yeast, Orm1 and Orm2 are mainly phosphorylated by Npr1 and Ypk1, respectively (Roelants et al., 2011; Sun et al., 2012; Shimobayashi et al., 2013). Besides ORMs, other polypeptides can also regulate the activity of SPT, namely, Tsc3 in yeast (Gable et al., 2000) and ssSPTa (68 amino acids) and ssSPTb (76 amino acids) in human (Han et al., 2009). The 56-amino acid ssSPTs, ssSPTa and ssSPTb, strongly stimulate Arabidopsis SPT activity when coexpressed with Arabidopsis LCB1 and LCB2a or 2b in a yeast *spt* null mutant (Kimberlin et al., 2013). Also, ssSPTa suppression lines increase the resistance to FB1, and the ssSPTa overexpression lines display strong sensitivity to FB1 by increasing or decreasing SPT activity (Kimberlin et al., 2013). In this study, the de novo biosynthesis of sphingolipids was activated due to loss of Arabidopsis ORM function. The isotope-labeled LCBs and ceramides of *orm1* amiR-*ORM2* accumulated significantly after 24 h of incubation in ^{15}N-labeled serine, relative to the wild type, which showed that ORM was indeed a negative regulator of SPT in Arabidopsis, like in human and yeast. Through a yeast two-hybrid system, BiFC experiments, and co-IP assays, we confirmed that Arabidopsis ORMs can directly bind with the Arabidopsis ssSPTs. Based on our data, we put forward two possible mechanisms for the function of ORMs (Figure 8). On the

one hand, ORM protein might bind to the SPT complex through the physical interaction with ssSPT and inhibit the enzyme activity of SPT, rather than changing its localization; on the other hand, the interaction between ORM and ssSPT might reduce the available ssSPTs that can interact with core LCB1/LCB2. We favor the first mechanism, in which ORM binds to the SPT complex with the ssSPT interaction, based on a recent study by Kimberlin et al. (2016). In addition, we observed that the ORMs and ssSPT localize in the ER, which could be the site where they interact (Figure 1; Supplemental Figure 6). Moreover, during FB1 treatment, *ORM* overexpression lines displayed strong resistance to FB1, the opposite effect to that of ssSPTa. Taking these results together, we speculate that ORMs could modulate sphingolipid levels by inhibiting the function of ssSPTs in Arabidopsis. When the ORMs are knocked out, SPT could be activated without changing its location, resulting in substantial accumulation of sphingolipids (Figure 8).

Like in humans and yeast, ORM proteins in Arabidopsis play an important role in maintaining the level of sphingolipids (Tafesse and Holthuis, 2010; Breslow et al., 2010; Liu et al., 2012). In this study, we analyzed the *ORM1* T-DNA insertion mutant *orm1* and the *ORM2* silencing line (amiR-*ORM2*). Under normal growth conditions, these plants showed no obvious differences compared with the wild type. However, the *orm1* amiR-*ORM2* plants exhibited premature senescence and considerable changes in sphingolipid contents, including multiple-fold increases in overall sphingolipids, especially in LCBs and ceramides. Among these, d18:0 and t18:0 LCB, the ceramide backbones containing long-chain fatty acids (C16), exhibited the largest changes. Measurements of the sphingolipid contents of *orm1* amiR-*ORM2* and wild-type rosettes at different developmental stages showed that prior to the onset of the early-senescence phenotype, the total LCBs, ceramides, and hydroxyceramides, mainly ceramide backbones containing dihydroxy LCBs and C16 fatty acids, increased in *orm1* amiR-*ORM2* plants compared with wild-type plants. These observations suggest that LCBs or ceramides may induce plant senescence and accumulate to threshold levels due to loss of ORM function.

Sphingolipids are involved in the regulation of plant responses to biotic and abiotic stresses. Our previous studies showed that the Arabidopsis neutral ceramidase mutant *ncer1* accumulates hydroxyceramides and is sensitive to oxidative stress (Li et al., 2015) and the ceramide kinase mutant *acd5* accumulates ceramides and is sensitive to *P. syringae* and *Botrytis cinerea* (Liang et al., 2003; Bi et al., 2014). In addition, the fatty acid α hydroxylase mutant *fah1 fah2* has a stronger resistance to Diplodia powdery mildew and Verticillium fungi (*Verticillium longisporum*) compared with the wild type (König et al., 2012). In this study, we found that plants with loss of ORM function are more resistant to MV and pathogen infection. This phenomenon could be attributed to the higher accumulation of LCBs in the ORMs mutants compared with the *acd5* and *fah1 fah2* mutants. Several previous studies reported that LCBs play an important role during abiotic and biotic stress (Peer et al., 2010; Saucedo-García et al., 2011; Li et al., 2015). LCBs can induce *MPK6* expression and programmed cell death by an MPK6-mediated signal transduction pathway (Saucedo-García et al., 2011). The expression of *MPK6* can be induced rapidly by Flg22, which mediates the pathogen-associated pattern-induced basal resistance (Galletti et al., 2011). Phytosphingosine content has been reported to rapidly escalate at two hours after *P. syringae* inoculation and is also involved in plant resistance (Peer et al., 2010). Our sphingolipid data also showed an increase in the

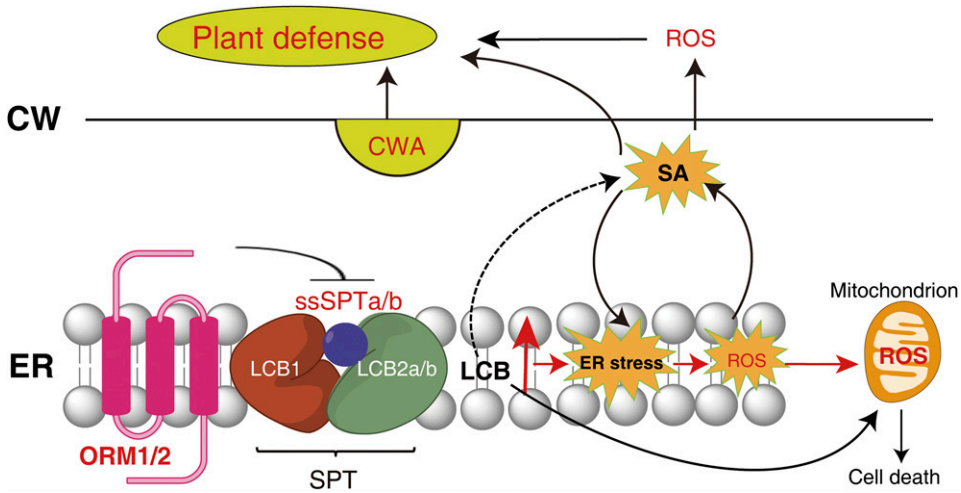

Figure 8. Model of ORM1- and ORM2-Mediated Sphingolipid Homeostasis and Plant Resistance.

The proposed model for ORM1 and ORM2 functions as negative regulators of de novo sphingolipid synthesis in Arabidopsis based on this study. SPT, localized on the ER, consists of LCB1, LCB2a/b, and ssSPTa/b and catalyzes the first step in sphingolipid biosynthesis. SPT demonstrates extremely low enzyme activity without ssSPTa/b (Kimberlin et al., 2013). We found that ORM1 and ORM2 inhibit the biosynthesis of LCB through physically interacting with ssSPTa/b. Moreover, in plants lacking ORM1 or ORM2, the profile of sphingolipids was enhanced, accompanied by a senescence phenotype and increased disease resistance. A possible mechanism related to defense in ORM1 and ORM2 loss-of-function plants is proposed. CW, cell wall; SA, salicylic acid; CWA, cell wall apposition. Red letters and arrows represent data in this study. The black dotted arrow represents our speculation.

phytosphingosine contents in plants with loss of ORM function, which leads to increased resistance against *P. syringae* infection. In addition, our TEM observation gives us another indication of the defense response in plants with decreased ORM1 or ORM2 (Figure 8), showing that active vesicular transport may be caused by perturbing the ORM-mediated sphingolipid homeostasis, and this may strengthen cell surface defenses (including formation of cell wall appositions and ROS production on the cell wall). Furthermore, based on the high transcript levels of resistance-related genes (*PR1*) in plants with loss of ORM function, and especially the upregulated ER stress-related genes (Liu and Howell, 2010) and expression of *PAD4*, *SID2*, and *NPR1* genes related to the SA pathway, we propose that loss of ORM function may affect SA biosynthesis, thereby affecting the plant's resistance to pathogens.

METHODS

Plant Materials and Growth Conditions

Wild-type *Arabidopsis thaliana* (Columbia, Col-0) and T-DNA insertion *orm* mutants (SALK_046054 and SAIL_1286_D09) from the ABRC (http://abrc.osu.edu/) were sown on soil after 3 d of stratification at 4°C, followed by cultivation in the greenhouse at 22°C and 50% relative humidity, 16 h light/8 h dark with 4800 to 6000 lux light intensity (PAK bulb, PAK090311).

To construct the *ORM1* and *ORM2* RNAi suppression vectors, the RS300 plasmid was employed to clone an artificial microRNA, as previously described (Schwab et al., 2006). The artificial microRNA was inserted into pCAMBIA1300 and fused with the 35S promoter and NOS terminator. The *ORM1* and *ORM2* overexpression constructs were generated using pCAMBIA1300 by inserting the open reading frame of *ORM1* or *ORM2*, the 35S promoter, and NOS terminator sequences. Finally, these constructs were transformed into the wild type using an *Agrobacterium tumefaciens* (EHA105)-mediated method. Transformed progenies were screened on 0.5× MS medium containing 0.25 mg/L hygromycin. Homozygous transgenic lines were isolated from the T3 generation for further study. All primers used for cloning are shown in Supplemental Table 1.

Phosphorylation Site Analysis of ORMs

For the analysis of potential phosphorylation sites presented in ORM proteins, the amino acid sequences of Arabidopsis ORM1 and ORM2 were submitted to the NetPhos 3.1 (http://www.cbs.dtu.dk/services/NetPhos/) and PhosPhAt 4.0 (http://phosphat.uni-hohenheim.de/phosphat.html) online tools, respectively (Blom et al., 2004; Durek et al., 2010).

Quantitative RT-PCR Analysis

Total RNA was extracted using the E.Z.N.A. plant RNA kit (R6827-01; Omega Bio-tek). For each sample, 1 μg RNA was reverse transcribed into cDNA using the Primescript RT reagent kit (Takara; DRR047A). Real-time PCR was performed with the SYBR Premix ExTaq kit (Takara; RR820L) according to the manufacturer's instructions and quantitatively analyzed with a Step One Plus real-time PCR system (ABI). The $2^{-\triangle\triangle}$CT method (Livak and Schmittgen, 2001) was used to determine the relative transcript level of target genes according to the expression level of *ACT2* (the internal control). All the experiments were performed in triplicate. The primers used in this study are listed in Supplemental Table 1. Unless otherwise mentioned, all chemicals were purchased from Sigma-Aldrich.

Subcellular Protein Localization

For subcellular protein localization, the $35S_{pro}$:*GFP*:*ORM1* and $35S_{pro}$:*GFP*:*ORM2* gene expression cassettes were constructed and inserted into pCAMBIA1300. Mesophyll protoplasts were isolated by the tape-Arabidopsis sandwich method and transformed by PEG-calcium mediated transfection (Wu et al., 2009). The transfected protoplasts were cultured under dim light (~300 lux) for 16 to 24 h at room temperature and observed by confocal microscopy (LSM-780; Carl Zeiss). The excitation/emission wavelengths were: 488 nm/500 to 530 nm for GFP, 561 nm/580 to 630 nm for mCherry, and 488 nm/650 to 750 nm for chlorophyll.

Sphingolipid Analysis

Measurement of sphingolipids was performed and the data were analyzed by a Shimadzu UFLC-XR coupled with a hybrid quadrupole time-of-flight mass spectrometer (AB SCIEX Triple TOF 5600+) using a Phenomenex Luna C8 column (150 mm × 2.0 mm, 3 μm). Briefly, 30 mg of lyophilized sample was homogenized. The internal standards (C17 base D-erythro-sphingosine and d18:1 C12:0-ceramide) were added and extracted with the isopropanol/hexane/water (55:20:25 v/v/v) and incubated at 60°C for 15 min. After centrifugation, the supernatants were dried and de-esterified in methylamine in ethanol/water (70:30 v/v) as described previously (Bi et al., 2014; Li et al., 2015; Wu et al., 2015). The sphingolipid species were analyzed using the software Multiquant (AB SCIEX).

Yeast Two-Hybrid Assay

Yeast two-hybrid analysis was conducted following the Matchmaker Gold Yeast Two-Hybrid System User Manual (Clontech). The full-length open reading frames of *ssSPTa* and *ssSPTb* were fused to the bait vector pGBKT7, and the full-length open reading frames of *ORM1* and *ORM2* were cloned into the prey vector pGADT7. Prey and bait vectors were transformed into the yeast strain Y2H Gold (Clontech), and yeast was grown on SD/-Trp-Leu medium for 3 d. Transformants were incubated at 30°C in a shaking incubator with SD/-Trp-Leu broth until OD_{600} = 1.0 was obtained and then tested on selective SD medium at 30°C for 5 d. Empty vectors were used as the negative control.

BiFC Assay

The full-length coding sequences of *ORM1* and *ORM2* were cloned into pSATN-nEYFP-C1, and full-length coding sequences of *ssSPTa* and *ssSPTb* were cloned into pSATN-cYFP-C1 (Citovsky et al., 2006). Protoplast isolation and transient expression were performed as described previously (Wu et al., 2009). Empty vectors were cotransformed as negative controls.

Co-IP Assay

Mesophyll protoplast isolation from 3- to 4-week-old Arabidopsis leaves and DNA transfection were performed as described previously (Wu et al., 2009). For the protocol, 100 μg of prey plasmids and 100 μg of bait plasmids were cotransfected into 1 mL protoplasts (5×10^5 cells). After expression of proteins for 12 h, protoplasts were pelleted and lysed in 200 μL of immunoprecipitation buffer (50 mM Tris-HCl, pH 7.5, 150 mM NaCl, 1 mM EDTA, 10% glycerol, 1% Triton X-100, and 13 Roche EDTA-free protease inhibitor cocktail) by vigorous vortexing. For each sample, 20 μL of lysate was saved as the input fraction. The remaining of the lysate was mixed with 300 μL immunoprecipitation buffer and vigorously vortexed. The clear lysate was centrifuged at 16,000*g* for 10 min at 4°C, and the supernatant was incubated with 20 μL of anti-Flag agarose resins (Sigma-Aldrich) for 4 h at 4°C. The resin was washed three times with immunoprecipitation buffer. The resins were boiled in 40 μL of SDS-PAGE loading buffer to obtain the eluate and prey proteins was detected by immunoblotting analysis using anti-Flag antibody and anti-GFP antibody (Cell Signal) at 1:2000 dilution. The immunoblot signal was visualized with the Clarity Western ECL substrate kit (Bio-Rad).

H_2O_2 Detection by $CeCl_3$ Staining and TEM Observation

For electron microscopy samples, ~25-d-old Arabidopsis rosette leaves from soil-grown plants were used. The histochemical cerium chloride method was used to detect H_2O_2 based on generation of cerium hydroxide, as described previously (Bi et al., 2014). The leaves were cut and incubated in 10 mM $CeCl_3$ dissolved in 50 mM MOPS buffer (pH 7.2) for 1 h. Control samples were incubated in MOPS buffer only. Samples were fixed in 2.5% (v/v) glutaraldehyde and 2% (v/v) paraformaldehyde in 0.1 M cacodylate buffer (pH 7.4). Samples were embedded in SPI-PON812 resin (SPI Supplies). Ultrathin sections were obtained on a microtome (Leica EM UC6) and examined without staining. The images were photographed using a transmission electron microscope (JEM-1400; JEOL) at an accelerating voltage of 120 kV.

Abiotic and Biotic Stress Treatments

The seeds of each line were sown on 0.5× MS medium supplemented with FB1 (0.5 μM) or MV (0.5 μM). After 2 to 3 d at 4°C in the dark, plates were transferred into an incubator with a 16-h-light/8-h-dark light regimen. Phenotypes were characterized and scored. For bacterial infection, leaves from 3-week-old plants were injected with the virulent *Pseudomonas syringae* strain DG3 at OD_{600} = 0.001 or with 10 mM $MgSO_4$ as a mock-inoculated control. Leaf discs were harvested for bacterial quantification at indicated days after inoculation as previous reports (Bi et al., 2014; Wu et al., 2015).

Accession Numbers

Sequence data from this article can be found in the Arabidopsis Genome Initiative or GenBank/EMBL databases under the following accession numbers: *ORM1* (At1G01230), *ORM2* (At5G42000), *ssSPTa* (At1g06515), *ssSPTb* (At2g30942), *LCB1* (At4g36480), *LCB2a* (At5g23670), *LCB2b* (At3g48780), *ACT2* (At3g18780), *TUBULIN* (At5G62690), *IRE1a* (At2G17520), *bZIP28* (At3G10800), *bZIP60* (At1G42990), *TBF1* (At4G36990), *PAD4* (At3g52430), *SID2* (At1g74710), *NPR1* (At1g64280), *PR1* (At2g14610), *orm1* (SALK_046054), and *orm2* (SAIL_1286_D09).

Supplemental Data

Supplemental Figure 1. Sequence alignment of the two Arabidopsis ORM proteins and expression of Arabidopsis *ORMs.*

Supplemental Figure 2. Transmembrane helices predicted in ORM1 and ORM2.

Supplemental Figure 3. Phenotypes and sphingolipid profiles in *orm1* and *ORM* transgenic plants.

Supplemental Figure 4. Comparison of major LCB and ceramide components between *orm1* amiR-*ORM2* and the wild type.

Supplemental Figure 5. Sphingolipid contents in wild-type and *orm1* amiR-*ORM2* plants at different developmental stages.

Supplemental Figure 6. Subcellular localization of ssSPT and biomolecular fluorescence complementation assay between ORM1 and ssSPTa.

Supplemental Figure 7. Subcellular localization of SPT in *orm1* amiR-*ORM2* plants.

Supplemental Table 1. List of primers used in this study.

ACKNOWLEDGMENTS

We thank Edgar Cahoon (University of Nebraska-Lincoln) for helpful discussion and Jian-Feng Li (Sun Yat-sen University) for assistance with co-IP experiments. This work was funded by the National Natural Science Foundation of China (31570255), the National Key Basic Science 973 program (2012CB114006), the Foundation of Guangzhou Science and Technology Project (201504010021), and the Fundamental Research Funds for the Central Universities (16lgjc74) to N.Y. and by the China Postdoctoral Science Foundation (2016M592575) to S.K.S.

AUTHOR CONTRIBUTIONS

N.Y., J.L., and J.-X.W. conceived and designed experiments. J.L., J.Y., C.R., K.-E.L., L.-Q.H., and H.-Y.Z. performed the experiments. J.L., J.Y., K.-E.L., J.-X.W., and N.Y. analyzed the data. N.Y, J.L., and S.K.S. wrote the article.

Received July 19, 2016; revised October 15, 2016; accepted December 1, 2016; published December 6, 2016.

REFERENCES

Berchtold, D., Piccolis, M., Chiaruttini, N., Riezman, I., Riezman, H., Roux, A., Walther, T.C., and Loewith, R. (2012). Plasma membrane stress induces relocalization of Slm proteins and activation of TORC2 to promote sphingolipid synthesis. Nat. Cell Biol. **14:** 542–547.

Bi, F.C., et al. (2014). Loss of ceramide kinase in Arabidopsis impairs defenses and promotes ceramide accumulation and mitochondrial H_2O_2 bursts. Plant Cell **26:** 3449–3467.

Blom, N., Sicheritz-Pontén, T., Gupta, R., Gammeltoft, S., and Brunak, S. (2004). Prediction of post-translational glycosylation and phosphorylation of proteins from the amino acid sequence. Proteomics **4:** 1633–1649.

Breslow, D.K. (2013). Sphingolipid homeostasis in the endoplasmic reticulum and beyond. Cold Spring Harb. Perspect. Biol. **5:** a013326.

Breslow, D.K., Collins, S.R., Bodenmiller, B., Aebersold, R., Simons, K., Shevchenko, A., Ejsing, C.S., and Weissman, J.S. (2010). Orm family proteins mediate sphingolipid homeostasis. Nature **463:** 1048–1053.

Brinkmann, V., Billich, A., Baumruker, T., Heining, P., Schmouder, R., Francis, G., Aradhye, S., and Burtin, P. (2010). Fingolimod (FTY720): discovery and development of an oral drug to treat multiple sclerosis. Nat. Rev. Drug Discov. **9:** 883–897.

Chen, M., Han, G., Dietrich, C.R., Dunn, T.M., and Cahoon, E.B. (2006). The essential nature of sphingolipids in plants as revealed by the functional identification and characterization of the Arabidopsis LCB1 subunit of serine palmitoyltransferase. Plant Cell **18:** 3576–3593.

Chen, M., Cahoon, E., Saucedo-García, M., Plasencia, J., and Gavilanes-Ruíz, M. (2009). Plant sphingolipids: structure, synthesis and function. In Lipids in Photosynthesis: Essential and Regulatory Functions, H. Wada and N. Murata, eds (Dordrecht, The Netherlands: Springer), pp. 77–116.

Citovsky, V., Lee, L.Y., Vyas, S., Glick, E., Chen, M.H., Vainstein, A., Gafni, Y., Gelvin, S.B., and Tzfira, T. (2006). Subcellular localization of interacting proteins by bimolecular fluorescence complementation in planta. J. Mol. Biol. **362:** 1120–1131.

Dietrich, C.R., Han, G., Chen, M., Berg, R.H., Dunn, T.M., and Cahoon, E.B. (2008). Loss-of-function mutations and inducible RNAi suppression of Arabidopsis LCB2 genes reveal the critical role of sphingolipids in gametophytic and sporophytic cell viability. Plant J. **54:** 284–298.

Durek, P., Schmidt, R., Heazlewood, J.L., Jones, A., MacLean, D., Nagel, A., Kersten, B., and Schulze, W.X. (2010). PhosPhAt: the Arabidopsis thaliana phosphorylation site database. An update. Nucleic Acids Res. **38:** D828–D834.

Gable, K., Slife, H., Bacikova, D., Monaghan, E., and Dunn, T.M. (2000). Tsc3p is an 80-amino acid protein associated with serine palmitoyltransferase and required for optimal enzyme activity. J. Biol. Chem. **275:** 7597–7603.

Galletti, R., Ferrari, S., and De Lorenzo, G. (2011). Arabidopsis MPK3 and MPK6 play different roles in basal and oligogalacturonide- or flagellin-induced resistance against *Botrytis cinerea.* Plant Physiol. **157:** 804–814.

Gururaj, C., Federman, R.S., and Chang, A. (2013). Orm proteins integrate multiple signals to maintain sphingolipid homeostasis. J. Biol. Chem. **288:** 20453–20463. Erratum. J. Biol. Chem. **290:** 1455.

Han, G., Gupta, S.D., Gable, K., Niranjanakumari, S., Moitra, P., Eichler, F., Brown, R.H., Jr., Harmon, J.M., and Dunn, T.M. (2009). Identification of small subunits of mammalian serine palmitoyltransferase that confer distinct acyl-CoA substrate specificities. Proc. Natl. Acad. Sci. USA **106:** 8186–8191.

Han, S., Lone, M.A., Schneiter, R., and Chang, A. (2010). Orm1 and Orm2 are conserved endoplasmic reticulum membrane proteins regulating lipid homeostasis and protein quality control. Proc. Natl. Acad. Sci. USA **107:** 5851–5856.

Hannun, Y.A., and Obeid, L.M. (2008). Principles of bioactive lipid signalling: lessons from sphingolipids. Nat. Rev. Mol. Cell Biol. **9:** 139–150.

Hjelmqvist, L., Tuson, M., Marfany, G., Herrero, E., Balcells, S., and Gonzàlez-Duarte, R. (2002). ORMDL proteins are a conserved new family of endoplasmic reticulum membrane proteins. Genome Biol. **3:** H0027.

Kiefer, K., Carreras-Sureda, A., García-López, R., Rubio-Moscardó, F., Casas, J., Fabriàs, G., and Vicente, R. (2015). Coordinated regulation of the orosomucoid-like gene family expression controls de novo ceramide synthesis in mammalian cells. J. Biol. Chem. **290:** 2822–2830.

Kimberlin, A.N., Majumder, S., Han, G., Chen, M., Cahoon, R.E., Stone, J.M., Dunn, T.M., and Cahoon, E.B. (2013). Arabidopsis 56-amino acid serine palmitoyltransferase-interacting proteins stimulate sphingolipid synthesis, are essential, and affect mycotoxin sensitivity. Plant Cell **25:** 4627–4639.

Kimberlin, A.N., Han, G., Luttgeharm, K.D., Chen, M., Cahoon, R.E., Stone, J.M., Markham, J.E., Dunn, T.M., and Cahoon, E.B. (2016). ORM expression alters sphingolipid homeostasis and differentially affects ceramide synthase activities. Plant Physiol. **172:** 889–900.

König, S., Feussner, K., Schwarz, M., Kaever, A., Iven, T., Landesfeind, M., Ternes, P., Karlovsky, P., Lipka, V., and Feussner, I. (2012). Arabidopsis mutants of sphingolipid fatty acid α-hydroxylases accumulate ceramides and salicylates. New Phytol. **196:** 1086–1097.

Lee, Y.J., Huang, X., Kropat, J., Henras, A., Merchant, S.S., Dickson, R.C., and Chanfreau, G.F. (2012). Sphingolipid signaling mediates iron toxicity. Cell Metab. **16:** 90–96.

Li, J., Bi, F.C., Yin, J., Wu, J.X., Rong, C., Wu, J.L., and Yao, N. (2015). An Arabidopsis neutral ceramidase mutant ncer1 accumulates hydroxyceramides and is sensitive to oxidative stress. Front. Plant Sci. **6:** 460.

Liang, H., Yao, N., Song, J.T., Luo, S., Lu, H., and Greenberg, J.T. (2003). Ceramides modulate programmed cell death in plants. Genes Dev. **17:** 2636–2641.

Lingwood, D., and Simons, K. (2010). Lipid rafts as a membrane-organizing principle. Science **327:** 46–50.

Liu, J.X., and Howell, S.H. (2010). Endoplasmic reticulum protein quality control and its relationship to environmental stress responses in plants. Plant Cell **22:** 2930–2942.

Liu, M., Huang, C., Polu, S.R., Schneiter, R., and Chang, A. (2012). Regulation of sphingolipid synthesis through Orm1 and Orm2 in yeast. J. Cell Sci. **125:** 2428–2435.

Livak, K.J., and Schmittgen, T.D. (2001). Analysis of relative gene expression data using real-time quantitative PCR and the 2(-Delta Delta C(T)) Method. Methods **25:** 402–408.

Markham, J.E., Molino, D., Gissot, L., Bellec, Y., Hématy, K., Marion, J., Belcram, K., Palauqui, J.C., Satiat-Jeunemaître, B., and Faure, J.D. (2011). Sphingolipids containing very-long-chain fatty acids define a secretory pathway for specific polar plasma membrane protein targeting in Arabidopsis. Plant Cell **23:** 2362–2378.

Modrak, D.E., Gold, D.V., and Goldenberg, D.M. (2006). Sphingolipid targets in cancer therapy. Mol. Cancer Ther. **5:** 200–208.

Moffatt, M.F., et al. (2007). Genetic variants regulating ORMDL3 expression contribute to the risk of childhood asthma. Nature **448:** 470–473.

Mizuno, S., Ogishima, S., Kitatani, K., Kikuchi, M., Tanaka, H., Yaegashi, N., and Nakaya, J. (2016). Network analysis of a comprehensive knowledge repository reveals a dual role for ceramide in Alzheimer's disease. PLoS One **11:** e0148431.

Msanne, J., Chen, M., Luttgeharm, K.D., Bradley, A.M., Mays, E.S., Paper, J.M., Boyle, D.L., Cahoon, R.E., Schrick, K., and Cahoon, E.B. (2015). Glucosylceramides are critical for cell-type differentiation and organogenesis, but not for cell viability in Arabidopsis. Plant J. **84:** 188–201.

Niles, B.J., Mogri, H., Hill, A., Vlahakis, A., and Powers, T. (2012). Plasma membrane recruitment and activation of the AGC kinase Ypk1 is mediated by target of rapamycin complex 2 (TORC2) and its effector proteins Slm1 and Slm2. Proc. Natl. Acad. Sci. USA **109:** 1536–1541.

Okamoto, H., Takuwa, N., Yokomizo, T., Sugimoto, N., Sakurada, S., Shigematsu, H., and Takuwa, Y. (2000). Inhibitory regulation of Rac activation, membrane ruffling, and cell migration by the G protein-coupled sphingosine-1-phosphate receptor EDG5 but not EDG1 or EDG3. Mol. Cell. Biol. **20:** 9247–9261.

Park, T.S., Panek, R.L., Rekhter, M.D., Mueller, S.B., Rosebury, W.S., Robertson, A., Hanselman, J.C., Kindt, E., Homan, R., and Karathanasis, S.K. (2006). Modulation of lipoprotein metabolism by inhibition of sphingomyelin synthesis in ApoE knockout mice. Atherosclerosis **189:** 264–272.

Peer, M., Stegmann, M., Mueller, M.J., and Waller, F. (2010). *Pseudomonas syringae* infection triggers de novo synthesis of phytosphingosine from sphinganine in *Arabidopsis thaliana*. FEBS Lett. **584:** 4053–4056.

Roelants, F.M., Breslow, D.K., Muir, A., Weissman, J.S., and Thorner, J. (2011). Protein kinase Ypk1 phosphorylates regulatory proteins Orm1 and Orm2 to control sphingolipid homeostasis in *Saccharomyces cerevisiae*. Proc. Natl. Acad. Sci. USA **108:** 19222–19227.

Saucedo-García, M., Guevara-García, A., González-Solís, A., Cruz-García, F., Vázquez-Santana, S., Markham, J.E., Lozano-Rosas, M.G., Dietrich, C.R., Ramos-Vega, M., Cahoon, E.B., and Gavilanes-Ruíz, M. (2011). MPK6, sphinganine and the LCB2a gene from serine palmitoyltransferase are required in the signaling pathway that mediates cell death induced by long chain bases in Arabidopsis. New Phytol. **191:** 943–957.

Schwab, R., Ossowski, S., Riester, M., Warthmann, N., and Weigel, D. (2006). Highly specific gene silencing by artificial microRNAs in Arabidopsis. Plant Cell **18:** 1121–1133.

Sentelle, R.D., Senkal, C.E., Jiang, W., Ponnusamy, S., Gencer, S., Selvam, S.P., Ramshesh, V.K., Peterson, Y.K., Lemasters, J.J., Szulc, Z.M., Bielawski, J., and Ogretmen, B. (2012). Ceramide targets autophagosomes to mitochondria and induces lethal mitophagy. Nat. Chem. Biol. **8:** 831–838.

Shi, C., Yin, J., Liu, Z., Wu, J.X., Zhao, Q., Ren, J., and Yao, N. (2015). A systematic simulation of the effect of salicylic acid on sphingolipid metabolism. Front. Plant Sci. **6:** 186.

Shi, L., Bielawski, J., Mu, J., Dong, H., Teng, C., Zhang, J., Yang, X., Tomishige, N., Hanada, K., Hannun, Y.A., and Zuo, J. (2007). Involvement of sphingoid bases in mediating reactive oxygen intermediate production and programmed cell death in Arabidopsis. Cell Res. **17:** 1030–1040.

Shimobayashi, M., Oppliger, W., Moes, S., Jenö, P., and Hall, M.N. (2013). TORC1-regulated protein kinase Npr1 phosphorylates Orm to stimulate complex sphingolipid synthesis. Mol. Biol. Cell **24:** 870–881.

Siow, D.L., and Wattenberg, B.W. (2012). Mammalian ORMDL proteins mediate the feedback response in ceramide biosynthesis. J. Biol. Chem. **287:** 40198–40204.

Summers, S.A., and Nelson, D.H. (2005). A role for sphingolipids in producing the common features of type 2 diabetes, metabolic syndrome X, and Cushing's syndrome. Diabetes **54:** 591–602.

Sun, Y., Miao, Y., Yamane, Y., Zhang, C., Shokat, K.M., Takematsu, H., Kozutsumi, Y., and Drubin, D.G. (2012). Orm protein phosphoregulation mediates transient sphingolipid biosynthesis response to heat stress via the Pkh-Ypk and Cdc55-PP2A pathways. Mol. Biol. Cell **23:** 2388–2398.

Tafesse, F.G., and Holthuis, J.C. (2010). Cell biology: A brake on lipid synthesis. Nature **463:** 1028–1029.

Teng, C., Dong, H., Shi, L., Deng, Y., Mu, J., Zhang, J., Yang, X., and Zuo, J. (2008). Serine palmitoyltransferase, a key enzyme for de novo synthesis of sphingolipids, is essential for male gametophyte development in Arabidopsis. Plant Physiol. **146:** 1322–1332.

Ternes, P., Feussner, K., Werner, S., Lerche, J., Iven, T., Heilmann, I., Riezman, H., and Feussner, I. (2011). Disruption of the ceramide synthase LOH1 causes spontaneous cell death in Arabidopsis thaliana. New Phytol. **192:** 841–854.

Wang, W., et al. (2008). An inositolphosphorylceramide synthase is involved in regulation of plant programmed cell death associated with defense in Arabidopsis. Plant Cell **20:** 3163–3179.

Wu, F.H., Shen, S.C., Lee, L.Y., Lee, S.H., Chan, M.T., and Lin, C.S. (2009). Tape-Arabidopsis Sandwich - a simpler Arabidopsis protoplast isolation method. Plant Methods **5:** 16.

Wu, J.X., Li, J., Liu, Z., Yin, J., Chang, Z.Y., Rong, C., Wu, J.L., Bi, F.C., and Yao, N. (2015). The Arabidopsis ceramidase AtACER functions in disease resistance and salt tolerance. Plant J. **81:** 767–780.

Zhang, H., Huang, L., Li, X.H., Ouyang, Z.G., Yu, Y.M., Li, D.Y., and Song, F.M. (2013). Overexpression of a rice long-chain base kinase gene OsLCBK1 in tobacco improves oxidative stress tolerance. Plant Biotechnol. **30:** 9–16.